

Engineered Bacterially Expressed Polypeptides: Assembly into Polymer Particles with Tailored Degradation Profiles**

Denison H. C. Chang, Angus P. R. Johnston, Kim L. Wark, Kerry Breheney, and Frank Caruso*

The development of nanoengineered therapeutic carriers has been the focus of extensive research over the last decade.^[1] The assembly of advanced delivery vehicles requires control over properties such as nanostructure, chemical functionality, and degradation behavior. Polypeptides represent an excellent class of materials to assemble into therapeutic carriers because they are naturally biodegradable and can be engineered to contain a variety of functional groups. Polypeptides have been incorporated into a wide array of polymeric carrier systems, including polymersomes,^[2] micelles,^[2b,c,3] layer-by-layer capsules,^[4] and single-component polymer particles (PPs) assembled from mesoporous silica (MS) spheres.^[5] To impart additional stability, these systems can be chemically crosslinked,^[4b,6] and we have previously shown for synthetic polymers that the degree of crosslinking affects the degradation rate of the materials.^[7] Conventional chemical techniques for the post-functionalization of polypeptides (such as carbodiimide coupling) do not afford control over the positions at which crosslinking occurs. However, such precision may be obtained by using bacterially synthesized peptides that are assembled into particulate systems, as bacterial expression enables precise control over the sequence—as well as molecular weight and chemical properties—of the polypeptides.^[8] This level of precision enables examination of complex assembled systems and the correlation of functional properties to be investigated without the influence of chemical and/or molecular weight distribution. The fabrication and investigation of such precisely defined materials have been the focus of an increasing number of studies in the last decade.^[9] In addition to expressing precisely defined polypeptides, bacteria reproduce at an exponential rate, enabling a large quantity of identical polypeptides to be

synthesized in a short time, thereby minimizing batch-to-batch variation and cost.

Herein, we report the bacterial synthesis of polypeptides with precise control over the position of cysteine residues for disulfide crosslinking, and the assembly of these polypeptides on MS spheres to form PPs. We investigate whether the degradation profiles of these PPs can be tailored by varying the percentage and position of the crosslinking groups on the assembled polypeptides. The degradation profiles of PPs constructed from polypeptide chains with precisely positioned crosslinking groups is also compared to PPs constructed from polypeptide chains with randomly positioned crosslinking groups (by chemical functionalization). To our knowledge, this work represents the first study on the effect of crosslinking position on the degradation of therapeutic carriers.

Bacterially derived polypeptide chains with glutamic acid backbones were used as building blocks for the assembly of PPs. Poly(L-glutamic acid) (PGA) has been reported to exhibit pH-reversible swelling and shrinking behavior,^[4b,10] and has been exploited in a wide range of biomedical studies without adverse side effects.^[11] Critical to the function of a drug delivery system is controlled degradation of the vehicle upon cell entry. In the current study, the coupling of thiol groups in cysteine allows stabilization of the PPs by the formation of disulfide linkages, which have been previously used to crosslink other delivery systems.^[12] The redox-active disulfide bonds can be reduced to thiol groups in simulated intracellular environments.^[13] The assembled PPs are promising for use as therapeutic carriers because they are stable under physiological conditions and degrade in simulated cytoplasmic environments.

To investigate the effect of crosslinking degree on the degradation rate of the PPs, we bacterially synthesized eight 100-residue-long cysteine-functionalized PGA (PGA_C) variants with varying percentages of cysteine (6–30%) (Scheme 1). The precise control over the amino acid sequence of a polypeptide chain afforded by bacterial synthesis resulted in monodispersed PGA_C, which was confirmed by matrix-assisted laser desorption/ionization-time of flight mass spectrometry (MALDI-TOF MS) (Supporting Information, Figure S2). A comparison of the MALDI-TOF MS spectra of the biosynthesized PGA_C (Figure S2a,b) with that of a commercially available PGA (Figure S2c) further highlights the level of control that bacterial synthesis affords over the molecular weight. Control over the sequences of the polypeptides through bacterial synthesis also allowed for the incorporation of cysteine residues with exact percentages and positions. The degree of thiolation was confirmed using NMR spectroscopy (Figure S3 and Table S4).

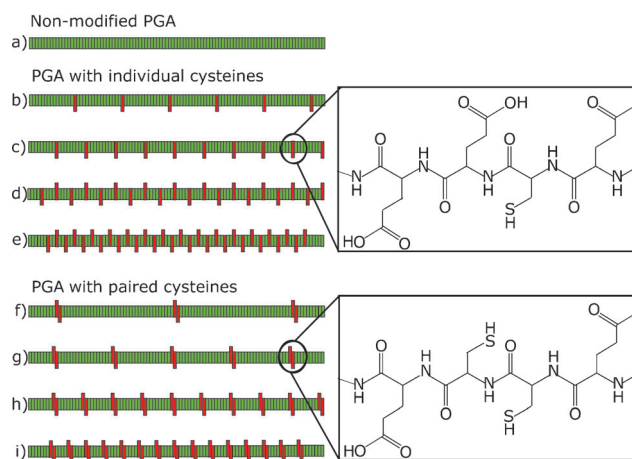
[*] D. H. C. Chang, Dr. A. P. R. Johnston, Prof. F. Caruso
Department of Chemical and Biomolecular Engineering
The University of Melbourne, Parkville, Victoria 3010 (Australia)
E-mail: fcaruso@unimelb.edu.au

Dr. K. L. Wark,^[†] K. Breheney
CSIRO, Molecular and Health Technologies
343 Royal Parade, Parkville, Victoria 3052 (Australia)

[†] Current address: Victorian Cancer Agency
12 Victoria Street, Carlton, Victoria 3053 (Australia)

[**] This work was supported by the Australian Research Council under the Federation Fellowship (FF0776078) and Discovery Project (DP0877360) schemes. We thank Dr. Henk Dam for his assistance with mass spectrometry, Dr. Christopher J. Ochs and Dr. Zhiyuan Zhu for their assistance with NMR analysis, and Dr. Lillian Lee for her assistance with CD spectroscopy.

Supporting information for this article is available on the WWW under <http://dx.doi.org/10.1002/anie.201106033>.



Scheme 1. The bacterially expressed and modified PGA: a) non-functionalized PGA; b–e) individually functionalized PGA with varying cysteine percentages, 6–30%; f–i) paired-cysteine-functionalized PGA, 6–30%. The polypeptides are denoted PGA_{xi} or PGA_{xp} . “x” refers to the percentage of cysteine groups, “i” to individually spaced cysteine groups, and “p” to paired cysteine groups.

The incorporation of cysteine residues into the polypeptide chain may result in conformational changes to the secondary structure of the polypeptides. These secondary structures were characterized using circular dichroism (CD) spectroscopy (Figure S4). Non-functionalized PGA showed the typical random coil structure in pH 7.4 phosphate-buffered saline (PBS) and α -helical structure in acidic conditions.^[14] However, all of the cysteine-modified PGA peptides showed CD spectra peaks, suggesting the partial formation of an α -helical structure.^[15] Although both series of PGA_{C} had a different structure to the non-modified PGA, the CD spectra of each PGA_{C} demonstrated no significant differences in the secondary structures among the functionalized derivatives, irrespective of the percentages and/or positions of the cysteines.

The similarity in structure and the precise control over molecular weight, enabled the effects of the positioning of crosslinking groups on the degradation rates to be examined by comparing paired cysteines (PGA_{xp}) and individually spaced residues (PGA_{xi}), where “x” refers to the percentage of cysteines. We demonstrate that spatial arrangement of the crosslinkers allows tuning of the PP degradation rate, which could be applied to tailoring cargo release. Further, we also compare the degradation rate of PPs assembled from PGA chemically modified by random functionalization of the carboxylic groups.

The bacterially derived PGA_{C} were assembled into PPs using sacrificial mesoporous particle templates. Mesoporous templates offer large surface areas and tunable pores,^[6a] and the resulting porous particle structure can be loaded with a high concentration of therapeutic cargo.^[5,6a] PP assembly involved two main steps. First, PGA_{C} was adsorbed onto aminated 5 μm diameter MS spheres, as this enables the negatively charged PGA_{C} to electrostatically adsorb onto the MS spheres. Next, the infiltrated polypeptides were cross-linked by the formation of disulfide bonds between cysteine residues using chloramine-T (CAT) as an oxidizing agent.

Dissolution of the MS spheres with hydrofluoric acid (HF) resulted in polypeptide-only PPs (Figure 1 a).

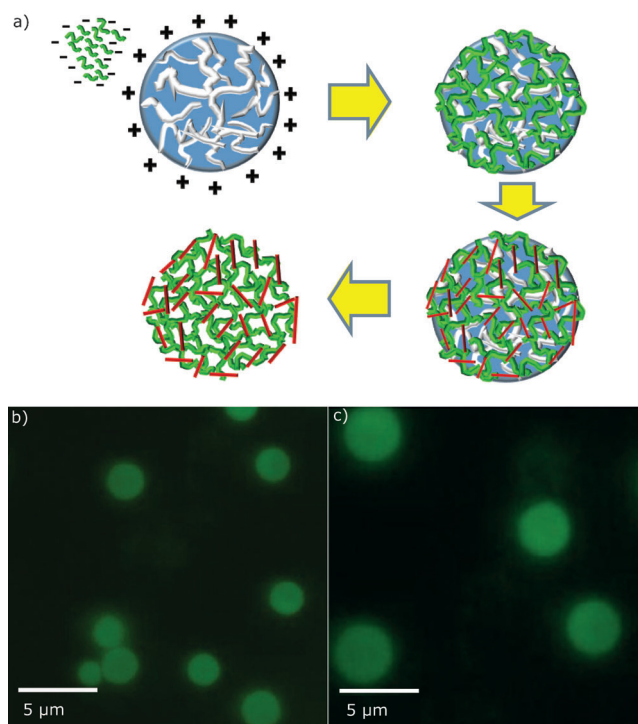


Figure 1. a) Negatively charged PGA_{xi} or PGA_{xp} were electrostatically adsorbed onto positively charged aminated MS spheres, followed by stabilization of the polypeptide assembly upon crosslinking the cysteine thiol groups with CAT. Dissolution of the silica template resulted in PGA_{xi} or PGA_{xp} particles. The polypeptides were fluorescently labeled with AF-488 before infiltration to enable visualization by fluorescence microscopy: b) $\text{PGA}_{10\text{i}}$ produced ca. 2 μm diameter PPs, whereas c) $\text{PGA}_{10\text{p}}$ produced ca. 3 μm diameter PPs.

Since there were no significant structural differences between the various PGA_{C} building blocks (Figure S4) that could influence the characteristics of the assembled PPs, differences of the PP system can be attributed to the percentage and/or positions of the cysteine crosslinking groups. Furthermore, despite the different cysteine percentage, the PGA_{xi} series demonstrated no notable differences in their adsorption onto MS spheres (Figure S5), suggesting similar amounts of material were available for assembly into PPs. After removal of the silica templates, $\text{PGA}_{6\text{i}}$ -infiltrated particles disassembled, suggesting that crosslinking was insufficient to retain the original structures. All other PGA_{C} peptides resulted in stable PPs upon template removal. PPs formed from $\text{PGA}_{6\text{p}}$ and $\text{PGA}_{10\text{i}}$ (Figure 1 b) shrunk to ca. 2 μm diameter structures, whereas $\text{PGA}_{10\text{p}}$ (Figure 1 c), $\text{PGA}_{20\text{i}}$, $\text{PGA}_{20\text{p}}$, $\text{PGA}_{30\text{i}}$, and $\text{PGA}_{30\text{p}}$ formed larger (ca. 3 μm diameter) spheres (Figure S6). The smaller-sized PPs may be a result of insufficient crosslinking, resulting in the loss of material.

Adsorption of similar amounts of peptide into the MS spheres was also confirmed by determining the concentration of free cysteine residues adsorbed into the MS spheres (using 5,5-dithio-bis-(2-nitrobenzoic acid) (DTNB); Figure S7). As

expected, MS spheres infiltrated with $\text{PGA}_{30\text{x}}$ had approximately 5 times the free thiol concentration of MS spheres infiltrated with $\text{PGA}_{6\text{x}}$ (Figure S7). After the addition of CAT and subsequent core removal, the concentration of free cysteine in all of the crosslinked systems decreased to just above the detection limit of free thiols. For example, the concentration of free thiols in the $\text{PGA}_{30\text{i}}$ system decreased from 1.2 fmol per particle prior to crosslinking to only 18 amol per particle after crosslinking and core dissolution. This suggests that the majority of the cysteine residues have crosslinked to form disulfide bonds.

Alexa Fluor 488 (AF-488) fluorescently labeled disulfide-crosslinked PPs constructed from the various PGA_{C} peptides were incubated in PBS for 60 min at 37°C and monitored using flow cytometry to investigate the stability of the particles under physiological conditions. As anticipated, the particles did not degrade. To study the degradation of the different PPs, the particles were incubated in 5 mM glutathione (GSH) for 60 min at 37°C to mimic intracellular reducing conditions.^[16] Degradation did not occur as a gradual erosion of the assembled polypeptides, which would be evidenced as a shift in the fluorescence intensity on the flow cytometry peaks. Instead, degradation of the PPs was seen by decreased particle counts, suggesting particles disassembled quickly once a critical degree of disulfide cleavage was reached (Figure S8).

Degradation of the PPs was analyzed by measuring the particle concentration over 60 min as a percentage of the initial particle concentration prior to incubation in GSH (Figure 2a and b). PPs assembled from PGA_{xi} (individually positioned cysteine) degraded rapidly within 5 min (Figure 2a). There were no significant differences in degradation profiles of PPs assembled from $\text{PGA}_{10\text{i}}$, $\text{PGA}_{20\text{i}}$, and $\text{PGA}_{30\text{i}}$, suggesting that when the cysteine residues were positioned individually, varying the cysteine content alone did not influence degradation. $\text{PGA}_{10\text{i}}$ -PPs degradation was also visualized using fluorescence microscopy at 0 and 15 min following the addition of GSH (Figure 2a). Degradation was observed as deformation of the PPs at 15 min. Similar degradation rates of PPs constructed from the three PGA_{C} peptides ($\text{PGA}_{10\text{i}}$, $\text{PGA}_{20\text{i}}$, and $\text{PGA}_{30\text{i}}$) may be due to low degrees of inter-chain crosslinking of $\text{PGA}_{20\text{i}}$ and $\text{PGA}_{30\text{i}}$. Since the thiol groups are evenly and individually spaced, intra-chain disulfide bonds may readily form, but these bonds would not play a role in stabilizing the assembled three-dimensional structures.

PPs assembled from PGA_{xp} peptides with cysteine percentages of 6–30% show that PPs with higher cysteine content degrade slower (Figure 2b). This indicates that when the crosslinking groups are paired, degradation profiles can be tailored by varying the percentage of the crosslinkers. To highlight the differences in degradation, the PP particle counts were compared after 30 min of incubation in GSH. PPs constructed using PGA_{xi} degraded more rapidly than those assembled from PGA_{xp} (Figure 2c), indicating that pairing the cysteine residues lowers the degradation rates of the PPs. Moreover, for the PPs assembled from paired cysteines with increasing cysteine content, the degradation rate decreased. The most notable difference was observed between particles

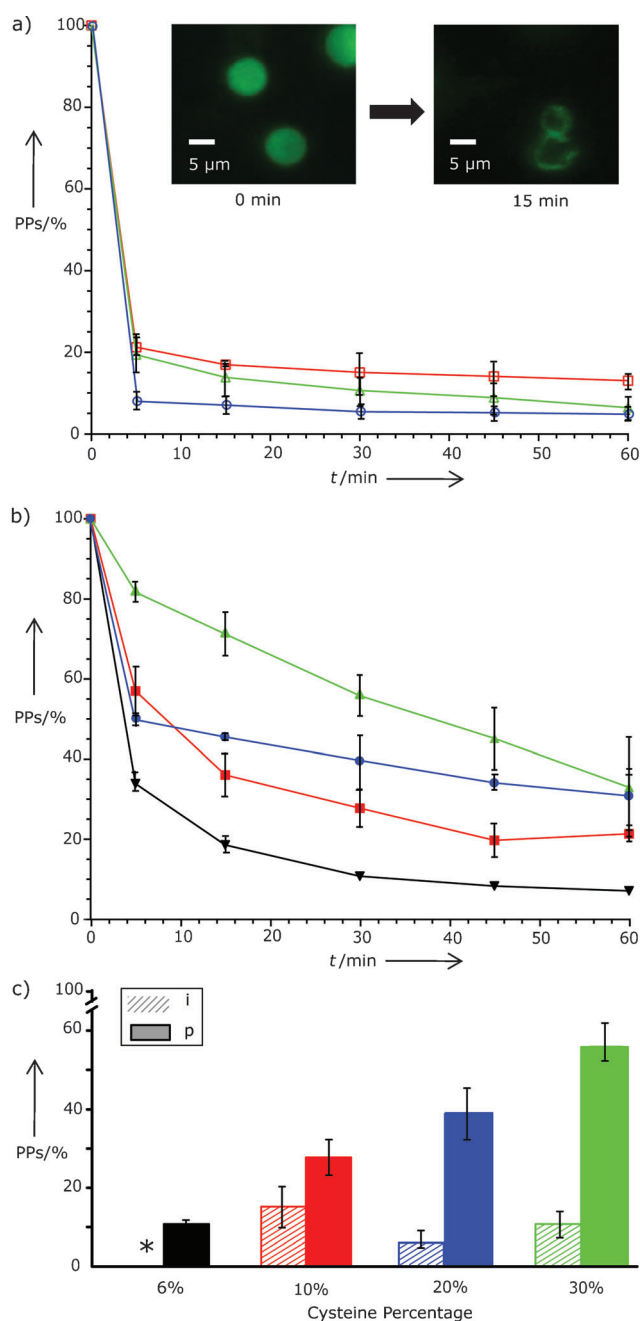


Figure 2. Degradation of PPs constructed from eight different derivatives of PGA_{C} (6% (black), 10% (red), 20% (blue), 30% (green); paired cysteines are represented by closed legends, and individual cysteines are represented by open legends) at physiological reducing conditions, 5 mM GSH at 37°C, as measured by flow cytometry and analyzed as a percentage of the initial particle count. a) Degradation of PPs constructed by PGA_{xi} was examined and PPs assembled from $\text{PGA}_{10\text{i}}$ were imaged using fluorescence microscopy at 0 and 15 min after incubation with 5 mM GSH (inset). b) The degradation of PPs constructed from PGA_{xp} was also examined, and c) the percentage of the remaining particles of all PPs at 30 min were observed. (* $\text{PGA}_{6\text{i}}$ did not assemble into stable PPs).

assembled from $\text{PGA}_{30\text{i}}$ or $\text{PGA}_{30\text{p}}$: $\text{PGA}_{30\text{p}}$ PPs had six and eight times more particles remaining after 30 and 60 min of incubation in GSH, respectively. This difference may be due

to the orientation of the paired cysteines on opposite sides of the peptide chain (Scheme 1), thus promoting the formation interpeptide bonds.

To examine differences between the degradation profiles of PPs constructed from polypeptides modified with either predetermined or random crosslinking group positions, PGA was functionalized with thiol-bearing-cystamine through 4-(4,6-dimethoxy-1,3,5-triazin-2-yl)-4-methylmorpholinium chloride (DMTMM) coupling (PGA_{10r}; “r” denotes random positioning of the crosslinking groups; 10% functionalization confirmed by NMR analysis; ¹H NMR (400 MHz, D₂O): δ = 1.95–2.20 (m, CH₂CH₂), 2.30–2.50 (m, CH₂CONH), 3.05–3.10 (br, CH₂SH), 3.55–3.75 (br, CONHCH₂), 4.15–4.30 ppm (br, NHCH₂CO)). Unmodified PGA was also adsorbed onto MS spheres and crosslinked by coupling cysteamine, a bifunctional amine that contains a disulfide bridge, to the carboxylic groups of the infiltrated PGA (PGA_{Xr}) through DMTMM coupling. Both chemical functionalization methods do not afford positional control, resulting in crosslinking of the polypeptides at random positions. Degradation of fluorescently labeled PPs assembled from PGA_{10i}, PGA_{10p}, PGA_{10r}, and PGA_{Xr} in 5 mM GSH at 37 °C was analyzed using flow cytometry. The rate of degradation of PPs assembled from PGA_{10r} and PGA_{Xr} was lower compared with that of PPs from the bacterially derived PGA_{10i} or PGA_{10p} peptides (Figure 3a). Differences in degradation profiles are highlighted by the PP particle counts after 30 min of incubation in GSH (Figure 3b). The degradation profile of PGA_{10r}-PPs was the slowest of the four types of PPs, followed by PPs constructed from PGA_{Xr}. The increased degradation rates of PPs constructed from PGA_{10i} or PGA_{10p} may be due to the ordered positions of the crosslinkers compared with both PPs constructed from PGA_{10r} or PGA_{Xr}, which are crosslinked at random positions.

In summary, we have demonstrated that the position of crosslinking groups affects the degradation rate of the assembled PP carriers: when the crosslinking moieties are individually and evenly spaced, varying the percentage of crosslinkers alone is insufficient to alter the degradation rate of the PPs. In contrast, when the crosslinkers are positioned in pairs, the PP degradation rate decreased as the percentage of crosslinkers increased. In addition, compared to PPs assembled from polypeptides with individually spaced crosslinkers, PPs constructed from polypeptides with paired crosslinkers degrade up to eight times slower in a simulated intracellular environment (after 60 min). This level of control over degradation rate is expected to translate to control over the release of encapsulated therapeutics in these systems. The results of this study are expected to underpin and provide new opportunities for designing delivery systems with controlled degradation properties and hence drug release rates.

Experimental Section

Bacterial expression of PGA_C was performed using the BL-21 strain of *E. coli*. The expressed polypeptides contained histidine tags at the N-terminus, which enabled purification of the product using a nickel-charged affinity column as histidine binds to it (see Supporting Information for more details). The purified PGA_C peptides, fluo-

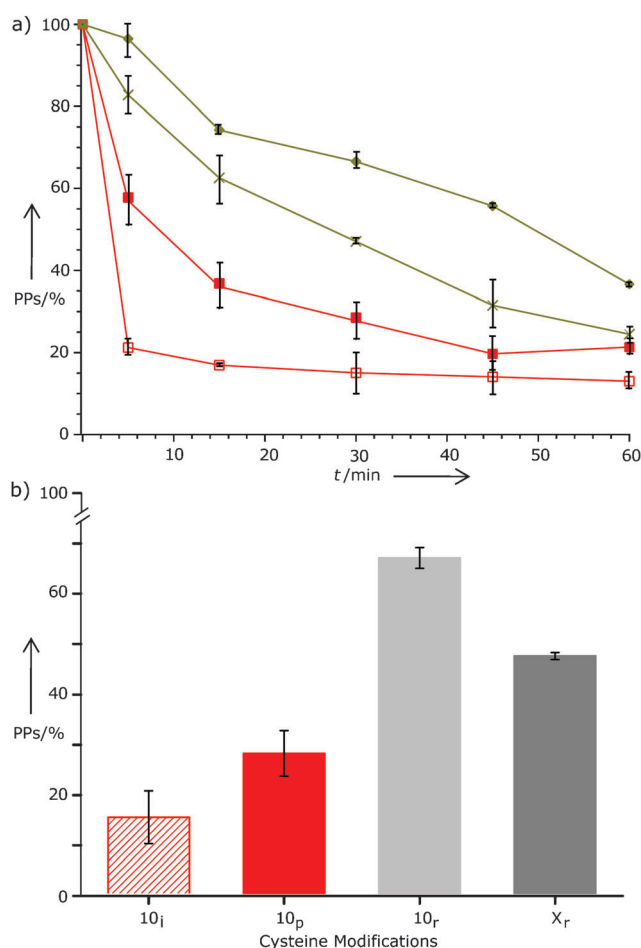


Figure 3. a) Degradation of PPs constructed from four different derivatives of 10% crosslinked polypeptides (□ PGA_{10i}, ■ PGA_{10p}, ◆ PGA_{10r}, × PGA_{Xr}) in 5 mM GSH at 37 °C was analyzed as the percentage of the initial particle count, and measured by flow cytometry at 0, 5, 15, 30, 45, and 60 min after incubation of the PPs in GSH. b) Percentage of remaining particles at 30 min after incubation in 5 mM GSH.

rescently labeled with AF-488, were adsorbed onto aminated 5.0 μ m-diameter MS spheres containing 100 nm pores. Adsorption was performed at room temperature for 48 h in 1 × Tris-EDTA (Tris = tris(hydroxymethyl)aminomethane, EDTA = ethylenediaminetetraacetic acid) buffer. 0.5M CAT was added to crosslink the PGA_C peptides by forming disulfide bonds from the thiol groups. The MS templates were then removed by ammonium fluoride (8M) buffered HF (2M), resulting in PGA_C-only PPs. Degradation of the PPs was performed in 5 mM GSH at 37 °C, and analyzed using flow cytometry and fluorescence microscopy (see Supporting Information for more details).

Received: August 26, 2011

Revised: October 13, 2011

Published online: November 23, 2011

Keywords: controlled degradation · drug delivery · peptides · polymer particles · positioned crosslinking

- [1] a) Y. Wang, A. D. Price, F. Caruso, *J. Mater. Chem.* **2009**, *19*, 6451; b) S. F. M. van Dongen, H. P. M. de Hoog, R. Peters, M. Nallani, R. J. M. Nolte, J. C. M. van Hest, *Chem. Rev.* **2009**, *109*,

- 6212; c) C. Minelli, S. B. Lowe, M. M. Stevens, *Small* **2010**, *6*, 2336; d) A. P. R. Johnston, G. K. Such, S. L. Ng, F. Caruso, *Curr. Opin. Colloid Interface Sci.* **2011**, *16*, 171.
- [2] a) H. R. Marsden, J. W. Handgraaf, F. Nudelman, N. Sommerdijk, A. Kros, *J. Am. Chem. Soc.* **2010**, *132*, 2370; b) W. Agut, A. Brulet, C. Schatz, D. Taton, S. Lecommandoux, *Langmuir* **2010**, *26*, 10546; c) X. J. Zhao, *Curr. Opin. Colloid Interface Sci.* **2009**, *14*, 340.
- [3] J. Wang, S. Y. Han, G. Meng, H. Xu, D. H. Xia, X. B. Zhao, R. Schweins, J. R. Lu, *Soft Matter* **2009**, *5*, 3870.
- [4] a) D. T. Haynie, N. Palath, Y. Liu, N. Pargaonkar, *Langmuir* **2005**, *21*, 1136; b) C. J. Ochs, G. K. Such, B. Städler, F. Caruso, *Biomacromolecules* **2008**, *9*, 3389.
- [5] a) J. Cui, Y. Wang, J. C. Hao, F. Caruso, *Chem. Mater.* **2009**, *21*, 4310; b) M. Vallet-Regí, F. Balas, D. Arcos, *Angew. Chem.* **2007**, *119*, 7692; *Angew. Chem. Int. Ed.* **2007**, *46*, 7548; c) M. Hartmann, *Chem. Mater.* **2005**, *17*, 4577.
- [6] a) Y. Wang, F. Caruso, *Adv. Mater.* **2006**, *18*, 795; b) W. Kim, J. Thevenot, E. Ibarboure, S. Lecommandoux, E. L. Chaikof, *Angew. Chem.* **2010**, *122*, 4353; *Angew. Chem. Int. Ed.* **2010**, *49*, 4257; c) B. C. Dash, S. Mahor, O. Carroll, A. Mathew, W. Wang, K. A. Woodhouse, A. Pandit, *J. Controlled Release* **2011**, *152*, 382.
- [7] A. L. Becker, A. N. Zelikin, A. P. R. Johnston, F. Caruso, *Langmuir* **2009**, *25*, 14079.
- [8] a) G. H. Zhang, M. J. Fournier, T. L. Mason, D. A. Tirrell, *Macromolecules* **1992**, *25*, 3601; b) S. J. M. Yu, V. P. Conticello, G. H. Zhang, C. Kayser, M. J. Fournier, T. L. Mason, D. A. Tirrell, *Nature* **1997**, *389*, 167.
- [9] a) L. Hartmann, H. G. Börner, *Adv. Mater.* **2009**, *21*, 3425; b) J.-F. Lutz, H. G. Börner, *Macromol. Rapid Commun.* **2011**, *32*, 113.
- [10] C. W. Zhao, X. L. Zhuang, P. He, C. S. Xiao, C. L. He, J. R. Sun, X. S. Chen, X. B. Jing, *Polymer* **2009**, *50*, 4308.
- [11] a) X. X. Wen, E. F. Jackson, R. E. Price, E. E. Kim, Q. P. Wu, S. Wallace, C. Charnsangavej, J. G. Gelovani, C. Li, *Bioconjugate Chem.* **2004**, *15*, 1408; b) T. J. Harris, J. J. Green, P. W. Fung, R. Langer, D. G. Anderson, S. N. Bhatia, *Biomaterials* **2010**, *31*, 998; c) P. Tryoen-Toth, D. Vautier, Y. Haikel, J. C. Voegel, P. Schaaf, J. Chluba, J. Ogier, *J. Biomed. Mater. Res.* **2002**, *60*, 657.
- [12] a) G. Saito, J. A. Swanson, K. D. Lee, *Adv. Drug Delivery Rev.* **2003**, *55*, 199; b) A. N. Zelikin, J. F. Quinn, F. Caruso, *Biomacromolecules* **2006**, *7*, 27.
- [13] a) B. Li, D. T. Haynie, *Biomacromolecules* **2004**, *5*, 1667; b) B. Li, D. T. Haynie, D. Janisch, *J. Nanosci. Nanotechnol.* **2005**, *12*, 2042.
- [14] M. Rinaudo, A. Domard, *J. Am. Chem. Soc.* **1976**, *98*, 6360.
- [15] G. Holzwarth, P. Doty, *J. Am. Chem. Soc.* **1965**, *87*, 218.
- [16] O. W. Griffith, *Free Radical Biol. Med.* **1999**, *27*, 922.